

Article

Satellite DNA in Neotropical Deer Species

Miluse Vozdova ^{1,*} , Svatava Kubickova ¹ , Natálie Martínková ² , David Javier Galindo ³ ,
Agda Maria Bernegossi ³ , Halina Cernohorska ¹ , Dita Kadlcikova ¹ , Petra Musilová ¹ ,
Jose Mauricio Duarte ³  and Jiri Rubes ¹

- ¹ Department of Genetics and Reproductive Biotechnologies, Central European Institute of Technology—Veterinary Research Institute, Hudcova 70, 621 00 Brno, Czech Republic; kubickova@vri.cz (S.K.); cernohorska@vri.cz (H.C.); kadlcikova@vri.cz (D.K.); musilova@vri.cz (P.M.); rubes@vri.cz (J.R.)
- ² Institute of Vertebrate Biology, Czech Academy of Sciences, Kvetna 8, 603 65 Brno, Czech Republic; martinkova@ivb.cz
- ³ Deer Research and Conservation Center (NUPECCE), School of Agricultural and Veterinarian Sciences, São Paulo State University (Unesp), 14884-900 Jaboticabal, Brazil; dgalindoh89@gmail.com (D.J.G.); agm.bernegossi@gmail.com (A.M.B.); mauricio.barbanti@unesp.br (J.M.D.)
- * Correspondence: vozdova@vri.cz; Tel.: +4205-3333-1422

Abstract: The taxonomy and phylogenetics of Neotropical deer have been mostly based on morphological criteria and needs a critical revision on the basis of new molecular and cytogenetic markers. In this study, we used the variation in the sequence, copy number, and chromosome localization of satellite I-IV DNA to evaluate evolutionary relationships among eight Neotropical deer species. Using FISH with satI-IV probes derived from *Mazama gouazoubira*, we proved the presence of satellite DNA blocks in peri/centromeric regions of all analyzed deer. Satellite DNA was also detected in the interstitial chromosome regions of species of the genus *Mazama* with highly reduced chromosome numbers. In contrast to *Blastocerus dichotomus*, *Ozotoceros bezoarticus*, and *Odocoileus virginianus*, *Mazama* species showed high abundance of satIV DNA by FISH. The phylogenetic analysis of the satellite DNA showed close relationships between *O. bezoarticus* and *B. dichotomus*. Furthermore, the Neotropical and Nearctic populations of *O. virginianus* formed a single clade. However, the satellite DNA phylogeny did not allow resolving the relationships within the genus *Mazama*. The high abundance of the satellite DNA in centromeres probably contributes to the formation of chromosomal rearrangements, thus leading to a fast and ongoing speciation in this genus, which has not yet been reflected in the satellite DNA sequence diversification.

Keywords: Cervidae; comparative cytogenetics; FISH; satellite DNA; sequencing



Citation: Vozdova, M.; Kubickova, S.; Martínková, N.; Galindo, D.J.; Bernegossi, A.M.; Cernohorska, H.; Kadlcikova, D.; Musilová, P.; Duarte, J.M.; Rubes, J. Satellite DNA in Neotropical Deer Species. *Genes* **2021**, *12*, 123. <https://doi.org/10.3390/genes12010123>

Received: 8 December 2020
Accepted: 16 January 2021
Published: 19 January 2021

Publisher's Note: MDPI stays neutral with regard to jurisdictional claims in published maps and institutional affiliations.



Copyright: © 2021 by the authors. Licensee MDPI, Basel, Switzerland. This article is an open access article distributed under the terms and conditions of the Creative Commons Attribution (CC BY) license (<https://creativecommons.org/licenses/by/4.0/>).

1. Introduction

Among large mammals, Neotropical deer (Cervidae, Pecora, Ruminantia, Artiodactyla) [1,2] represent an interesting group of species still lacking comprehensive scientific data. Their taxonomy has been established mostly on the basis of morphology indicating a need for its critical revision and a future systematic research [3,4]. Neotropical deer involve genera *Pudu*, *Mazama*, *Hippocamelus*, *Blastocerus*, *Ozotoceros*, and *Odocoileus* grouped in the tribe Rangiferini, subfamily Capreolinae [4,5]. As in other Cervidae, a variety of karyotypes has been observed in Neotropical deer, ranging from $2n = 70$ in *Mazama gouazoubira* or *Odocoileus virginianus*, to $2n = 32-34 + Bs$ in *Mazama bororo* [6,7]. The $2n = 70$ karyotype considered to reflect cervid ancestral karyotype has derived from the hypothetical ancestral karyotype of Pecora ($2n = 58$) by six chromosome fissions [6,8,9]. However, a series of evolutionary chromosome rearrangements occurred in many deer taxa, which led to a significant diversification of their karyotypes [9]. As with the other Neotropical deer species, a rapid karyotype evolution has been observed in *Mazama americana*, a taxon grouping several cryptic species currently classified as cytotypes on the basis of their karyotype differences

and geographical distribution and reported as *M. americana* species complex [4,10–12]. There is no doubt that the taxonomy and phylogenetics of the Neotropical deer would benefit from new approaches and utilization of new molecular markers.

A useful source of information can be found in satellite DNA, which consists of rapidly evolving, tandemly organized repetitive sequences, and might serve, to some extent, as molecular cytogenetic marker to trace individual and species origin and phylogeny. Satellite DNA located in centromeres and pericentromeric chromosome regions probably represents a structure linked to centromeric functions and chromosome segregation [13–16]. However, the functional roles of satellite DNA have not been fully elucidated yet. It is known that despite the relative uniformity of monomer lengths within satellite DNA families, they often show variations in sequence, copy numbers, and chromosome distribution even among related species [13,17], which can be used in phylogenetic studies [16,18–27].

Six satellite DNA families were described in Cervidae so far, of which satI–satIV were characterized in terms of sequence and chromosomal distribution in a number of Eurasian and North American cervid species [24,28–34]. However, there is a complete lack of data on satellite DNA sequences and their chromosome distribution in deer inhabiting South America. The sole exception is *O. virginianus*, a species spread throughout the American continent, in which a representative of its northern population has been under study recently [24].

In this study, we isolated four main groups of cervid satellite DNA sequences (satI–IV) in eight Neotropical deer species: *Mazama gouazoubira*, *Mazama nemorivaga*, *Mazama nana*, *Mazama bororo*, *M. americana*, *Blastocerus dichotomus*, *Ozotoceros bezoarticus*, and *O. virginianus* of South American origin. We performed intra- and inter-species comparisons of the obtained satellite DNA sequences and their physical localization on metaphase chromosomes using fluorescence in situ hybridization (FISH). We also searched the obtained sequences for a presence of the 17-bp binding motif for the CENP-B centromeric protein. Finally, we reconstructed phylogenetic trees of the satellite DNA sequences and compared them with the *mt-cyb* gene phylogeny to infer the evolutionary relationships among Neotropical deer species and their position within Cervidae.

2. Material and Methods

2.1. Species and Samples

Fibroblast tissue cultures prepared according to standard techniques from skin samples of eight Neotropical deer species and available at NUPECCE (Jaboticabal, Brazil) were used in this study for DNA isolation and FISH. No animals were euthanized in this study. The samples are listed in Table 1. To expand our knowledge on satellite DNAs in Cervidae, we also performed an analysis of partial satIII DNA sequence in eight Old world deer species (see Table 1) still missing data on satIII DNA sequence variability. Genomic DNA obtained previously [24] from peripheral lymphocytes was used for the analysis. Taxonomic nomenclature published by Groves and Grubb (2011) was used [5].

Table 1. Species analyzed in this study.

| Species | Latin Name | Abbr. ^a | 2n |
|--|--------------------------------|--------------------|--------------|
| Brown brocket deer | <i>Mazama gouazoubira</i> | MGO | 2n = 70 + B |
| Amazonian brown brocket deer | <i>Mazama nemorivaga</i> | MNE | 2n = 69 + B |
| Brazilian dwarf brocket deer | <i>Mazama nana</i> | MNA | 2n = 39 + Bs |
| Small red brocket deer | <i>Mazama bororo</i> | MBO | 2n = 33 + Bs |
| Red brocket deer-cytotype Paraná | <i>Mazama americana</i> | MAM-PR | 2n = 53 + Bs |
| Red brocket deer-cytotype Santarém | <i>M. americana</i> | MAM-SA | 2n = 51 + Bs |
| Red brocket deer-cytotype Juína | <i>M. americana</i> | MAM-JU | 2n = 45 + Bs |
| Red brocket deer-neotype from Roraima ^b | <i>M. americana</i> | MAM-RR | 2n = 46 + Bs |
| Marsh deer | <i>Blastocercus dichotomus</i> | BDI | 2n = 66 |
| Pampas deer | <i>Ozotoceros bezoarticus</i> | OBE | 2n = 68 |
| White-tailed deer of Brazilian origin | <i>Odocoileus virginianus</i> | OVI | 2n = 70 |
| Red deer | <i>Cervus elaphus</i> | CEL | 2n = 68 |
| Fallow deer | <i>Dama dama</i> | DDA | 2n = 68 |
| Eld's deer | <i>Rucervus eldii</i> | REL | 2n = 58 |
| Chinese muntjac | <i>Muntiacus reevesi</i> | MRE | 2n = 46 |
| Roe deer | <i>Capreolus capreolus</i> | CCA | 2n = 70 |
| Reindeer | <i>Rangifer tarandus</i> | RTA | 2n = 70 |
| Moose | <i>Alces alces</i> | AAL | 2n = 68 |
| White-tailed deer of North American origin | <i>Odocoileus virginianus</i> | OVI-N | 2n = 70 |

^a Abbreviation; ^b An animal from the region Roraima cytogenetically similar to the previously described neotype [10] but showing a heterozygous centric fission.

2.2. Satellite DNA Isolation

Genomic DNA was obtained from fixed suspensions of cultured fibroblasts of the available Neotropical deer using the QIAamp DNA Blood Mini Kit (Qiagen, Hilden, Germany) after washing in PBS. Satellite DNA was isolated from the genomic DNA by PCR amplification using previously published primer sets [24] (Table S1). SatI, satII, and satIV DNA sequences were isolated from all Neotropical deer species. SatIII DNA was obtained only from *M. gouazoubira*, and the satIII DNA internal fragment (satIII-part) was isolated from all remaining Neotropical and Old-World deer samples available for this study. All PCR reactions were performed using Hot Start Combi PPP Master Mix (Top-Bio, Prague, Czech Republic) according to the manufacturer's instructions. The obtained PCR products were cloned into the pDrive Cloning Vector (Qiagen, Hilden, Germany). Four different clones of each of satI, satII, satIII-part, and satIV DNA were selected in each species on the basis of their Hae III RFLP patterns (recognition site GG*CC) and subjected to sequencing.

2.3. Sequence Analysis

All satellite DNA sequences obtained in this study were screened for interspersed repeats using RepeatMasker (<http://www.repeatmasker.org>). The GC content was calculated using DNA/RNA GC Content Calculator (<http://www.endmemo.com>). All satellite sequences were also screened for a presence of the 17 bp CENP-B binding motif (NTTCGNNNNANNCGGN) and the satI for the 31-bp subrepeat unit motif [35,36] using FIMO (version 5.1.0) software (<http://meme-suite.org>) [37]. The satellite DNA sequences obtained in this study were compared to cervid satellite sequences available in the NCBI database using BLASTN (<https://blast.ncbi.nlm.nih.gov>) and BLAST2 software was used to assess the sequence homology.

2.4. FISH

Cloned satI, satII, satIII, and satIV DNA of *M. gouazoubira* were labelled with Orange- or Green-dUTP (Abbott, Abbott Park, IL, USA) using Nick Translation Reagent Kit (Abbott) to serve as probes for comparative FISH. FISH was performed using standard protocols [19]. Hybridization signals were examined using Zeiss Axio Imager.Z2 fluorescence microscope (Carl Zeiss Microimaging GmbH, Jena, Germany) equipped with appropriate fluorescent filters and the Metafer Slide Scanning System (MetaSystems, Altlusheim, Germany).

Images of well-spread metaphase cells were captured and analyzed using ISIS3 software (MetaSystems).

2.5. Phylogenetic Analysis

Multiple sequence alignments were constructed in MAFFT 7.474 [38] using the L-INS-i algorithm [39] for each satellite sequence separately. Alignments of cervid satellite DNA contain 1–8% of gaps [24], and gaps can influence phylogenetic reconstruction [40]. To capture phylogenetic information in gaps, the indels in the satI-IV alignments were recoded to presence/absence data and used as a partition in phylogenetic reconstruction [22]. For the indel partition, gaps in a sequence were coded as 1, and all nucleotides were coded as 0. Optimal substitution models for DNA sequences were selected with the smart model selection algorithm 1.8.4 based on the Bayesian Information Criterion that utilized likelihood estimation implemented in PhyML 3.3 [41,42]. The phylogenetic trees were reconstructed in MrBayes 3.2 [43] in the partitioned analysis, capturing the DNA sequence variation and the phylogenetic information in the indels. The Markov Chains Monte Carlo (MCMC) were run for 2 million generations, sampled every thousandth generation. Two runs of four MCMC were run to ascertain efficient treespace search and check for convergence, following discarding 30% of initial samples as burn-in. The analyses were considered converged when the average standard deviation of split frequencies was <0.01 at the end of the run, potential scale reduction factors were ≈ 1.000 for each model parameter and frequency of swaps between neighboring chains was between 0.3 and 0.7. The trees were visualized in R [44] with help from packages ape [45], treeio [46], phytools [47], and RColorBrewer [48], where nodes with posterior probability ≥ 0.95 were considered supported. The trees were rooted at midpoint.

We downloaded cervid reference sequences of the *mt-cyb* gene from the NCBI database to reconstruct a phylogenetic tree from a mitochondrial marker and to compare the satDNA and mtDNA phylogenies. The analysis was performed analogically to the analysis of satDNA sequences, with the difference that the mtDNA marker did not contain gaps and the phylogeny was reconstructed from a single partition containing the DNA sequences.

3. Results

3.1. Sequence Analysis

In this study, newly obtained satI, satII, satIII-part, and satIV DNA sequences were analyzed in the Neotropical deer species including different *M. americana* cytotypes. The PCR product lengths, GC content, and sequence similarities among the individual satellite DNA clones are displayed in Table 2. Moreover, the satIII-part sequence was isolated and analyzed in *C. elaphus*, *D. dama*, *R. eldii*, *M. reevesi*, *C. capreolus*, *R. tarandus*, and *A. alces*. All satellite DNA sequences obtained in this study were deposited in the NCBI database (accession numbers MW273496–MW273692).

Using RepeatMasker, we did not find any SINE, LINE, or LTR elements in the analyzed satI, satII, and satIV DNA sequences. In all analyzed species, the predicted CENP-B binding motif was detected in the satII DNA starting at position 145–148 bp (Table S2). Eighteen to 21 copies of the 31-subrepeat unit motif were revealed in the satI DNA sequences (Table 2). The sequences of the 31-bp subrepeat unit showed a substantial intra- and interspecies variability. A higher similarity was observed between the subrepeat sequences in a particular satI monomer position in different species than among the subrepeat sequences in the same satI monomer. The 31-bp subrepeat sequence variance and its positions in the satI sequence in the analysed Neotropical deer are shown in Table S3.

Sequence similarity among satellite DNAs of Neotropical deer, Capreolinae, and Cervinae was compared using both sequences obtained in this study, and those available in the NCBI database (Table 3). SatI DNA sequences showed the highest intra- and interspecies variability. A high intra- and interspecies satellite DNA sequence similarity was observed in satII-satIV, even when the Neotropical deer satellite DNA was compared with sequences previously published in Capreolinae and Cervinae (Table 3).

Table 2. Characteristics of the satI-IV sequences based on four clones of each satellite DNA analyzed in each sample of Neotropical deer (see text for abbreviations of species names).

| Species | SatI | | | | SatII | | | SatIII | | | SatIV | | |
|---------|-------------|----------------|----------------|--------------------|-------------|----------------|----------------|-------------|----------------|----------------|-------------|----------------|----------------|
| | Length (bp) | GC Content (%) | Similarity (%) | No. of 31-bp Units | Length (bp) | GC Content (%) | Similarity (%) | Length (bp) | GC Content (%) | Similarity (%) | Length (bp) | GC Content (%) | Similarity (%) |
| MGO | 910 | 51 | 96–99 | 19 | 579–581 | 67 | 97–99 | 583 | 53–56 | 89–98 | 727 | 45 | 97–99 |
| MNE | 910–913 | 51–53 | 76–92 | 19 | 578–580 | 65–67 | 92–96 | 580–583 | 55–58 | 90–93 | 726–727 | 44–45 | 96–99 |
| MNA | 904–919 | 46–51 | 75–84 | 20 | 575–579 | 64–67 | 90–93 | 579–583 | 56–59 | 89–97 | 727–728 | 45–46 | 98–99 |
| MBO | 910–917 | 49–51 | 76–92 | 18 | 578–579 | 64–66 | 92–94 | 579–583 | 55–58 | 90–94 | 727 | 45 | 99–100 |
| MAM_PR | 904–913 | 47–54 | 75–85 | 19 | 579 | 65–67 | 94–97 | 579–583 | 56–59 | 90–98 | 727 | 45 | 98–99 |
| MAM_SA | 904–910 | 47–51 | 72–94 | 18 | 578–579 | 64–67 | 92–98 | 581–583 | 56–59 | 90–95 | 727 | 44–46 | 97–99 |
| MAM_JU | 909–917 | 49–53 | 74–94 | 18 | 579–581 | 66–67 | 92–95 | 578–583 | 56–60 | 90–96 | 726–727 | 45–46 | 96–99 |
| MAM_RR | 908–910 | 51–52 | 77–98 | 20 | 575–579 | 64–67 | 93–96 | 580–583 | 54–59 | 86–93 | 727 | 45 | 97–99 |
| BDI | 911–919 | 48–50 | 77–80 | 21 | 579–580 | 63–67 | 88–98 | 579–584 | 56 | 92–97 | 726–737 | 45 | 93–97 |
| OBE | 911–917 | 48–51 | 76–98 | 18 | 580 | 67–68 | 96–99 | 582–583 | 55–58 | 91–99 | 727 | 45–46 | 92–99 |
| OVI | 907–915 | 48–51 | 74–99 | 19 | 578–579 | 66–67 | 97–98 | 581–584 | 55–56 | 94–97 | 727 | 44–46 | 95–99 |

Table 3. Satellite DNA sequence similarity among Neotropical deer, Capreolinae, and Cervinae (Cervini and Muntjacini).

| Species | SatI | | | SatII | | | SatIII-Partial | | | SatIV | | |
|---------|------------------|-------------|----------|------------------|-------------|----------|------------------|-------------|----------|------------------|-------------|----------|
| | Neotropical Deer | Capreolinae | Cervinae |
| MGO | 75–99 | 76–81 | 79–83 | 88–99 | 77–97 | 77–84 | 85–99 | 83–95 | 87–93 | 93–99 | 93–96 | 85–97 |
| MNE | 71–99 | 73–89 | 76–83 | 86–99 | 77–97 | 75–84 | 86–99 | 85–98 | 89–93 | 92–99 | 92–96 | 85–97 |
| MNA | 71–99 | 69–80 | 73–83 | 85–97 | 73–95 | 75–82 | 87–99 | 85–98 | 89–94 | 93–99 | 93–96 | 85–97 |
| MBO | 73–99 | 71–80 | 73–83 | 87–97 | 76–95 | 75–82 | 86–99 | 85–98 | 89–94 | 93–99 | 93–96 | 85–97 |
| MAM_PR | 72–99 | 73–89 | 74–83 | 87–99 | 77–96 | 76–84 | 87–99 | 85–98 | 89–94 | 93–99 | 93–96 | 85–96 |
| MAM_SA | 72–99 | 72–86 | 74–83 | 87–99 | 76–97 | 74–84 | 87–97 | 84–95 | 88–93 | 93–99 | 93–96 | 85–97 |
| MAM_JU | 72–99 | 70–86 | 73–83 | 86–97 | 76–96 | 74–83 | 88–99 | 85–98 | 89–94 | 93–99 | 93–96 | 85–97 |
| MAM_RR | 72–99 | 74–88 | 76–83 | 86–97 | 74–96 | 75–83 | 85–97 | 83–92 | 86–93 | 93–99 | 93–97 | 85–97 |
| BDI | 73–95 | 72–80 | 75–83 | 85–98 | 75–97 | 72–84 | 85–93 | 85–92 | 89–94 | 91–98 | 92–96 | 84–96 |
| OBE | 73–96 | 72–81 | 75–83 | 88–98 | 78–97 | 76–84 | 86–97 | 85–92 | 89–94 | 92–97 | 92–96 | 84–95 |
| OVI | 72–92 | 72–87 | 73–84 | 79–98 | 79–98 | 77–85 | 86–98 | 85–95 | 89–93 | 93–98 | 93–97 | 85–97 |

3.2. FISH

Probes for satI, satII, satIII, and satIV DNA obtained from *M. gouazoubira* were used for comparative FISH in the 11 Neotropical deer samples. The FISH results are summarized in Table 4 and displayed in Figures 1–4.

Table 4. Fluorescence in situ hybridization (FISH) patterns of the MGO satI-IV probes in Neotropical deer.

| Species | 2n | FN | B | SatI | SatII | SatIII | SatIV |
|---------|----|----|---|------------------------------------|------------------------------------|------------------------------|------------------------------------|
| MGO | 70 | 70 | + | all autosomes, X, Bs | all autosomes, X | a single autosome, weak | all autosomes, X |
| MNE | 69 | 72 | + | all autosomes, X, Bs | all autosomes, X | a few autosomes, weak | all autosomes |
| MNA | 39 | 58 | + | all autosomes, X, Bs, interstitial | all autosomes, X, interstitial | a few autosomes, weak | all autosomes, X, Bs, interstitial |
| MBO | 33 | 46 | + | all autosomes, X, Bs, interstitial | all autosomes, X, Bs, interstitial | a few autosomes, weak | most autosomes, X, interstitial |
| MAM PR | 53 | 56 | + | all autosomes, X, Bs, interstitial | all autosomes, X | a few autosomes, weak | all autosomes, X, interstitial |
| MAM SA | 51 | 56 | + | all autosomes, X, Bs, interstitial | all autosomes, X | a few autosomes, weak | all autosomes, interstitial |
| MAM JU | 45 | 48 | + | all autosomes, X, Bs, interstitial | all autosomes, X | a few autosomes, weak | all autosomes, X, interstitial |
| MAM RR | 46 | 51 | + | all autosomes, X, Bs, interstitial | all autosomes, X | a few autosomes, weak | all autosomes, interstitial |
| BDI | 66 | 74 | - | all autosomes, X | all autosomes, X | a few autosomes, big or weak | a few autosomes, big or weak |
| OBE | 68 | 74 | - | all autosomes, X | all autosomes, X | a few autosomes, weak | a few autosomes |
| OVI | 70 | 74 | - | all autosomes, X | all autosomes, X | a few autosomes, weak | a few autosomes |

In general, the MGO satI and satII probe produced centromeric signals on all autosomes (both acrocentric and bi-armed) and on the X chromosome in all analysed Neotropical deer (Figures 1 and 2). In all animals with B chromosomes, the satI probe also marked Bs. Moreover, the satI probe produced interstitial signals on one or more chromosomes in *M. nana*, *M. bororo* and in all four analyzed cytotypes of *M. americana*. Signals of the satII probe were also observed interstitially in *M. nana* and *M. bororo* and on B chromosomes in *M. bororo*. Examples of the interstitial signals and signals on B chromosomes are displayed in detail in Figure 2.

Using the MGO satIII probe, none or only weak subcentromeric signals were detected in the Neotropical Cervidae. The only exception was *B. dichotomus* showing also large signals on several autosomes (Figure 3).

The MGO satIV probe hybridized to large regions of centromeric heterochromatin of all chromosomes in most Neotropical deer species and produced also interstitial signals in *M. bororo* and in all *M. americana* cytotypes. In addition, B chromosomes were marked in *M. nana* (Figures 2 and 4). A different pattern was observed in *B. dichotomus*, *O. bezoarticus*, and the Brazilian *O. virginianus*, only showing very weak centromeric signals of the satIV

probe on a few autosomes together with several intense signals in *B. dichotomus* and *O. bezoarticus*.

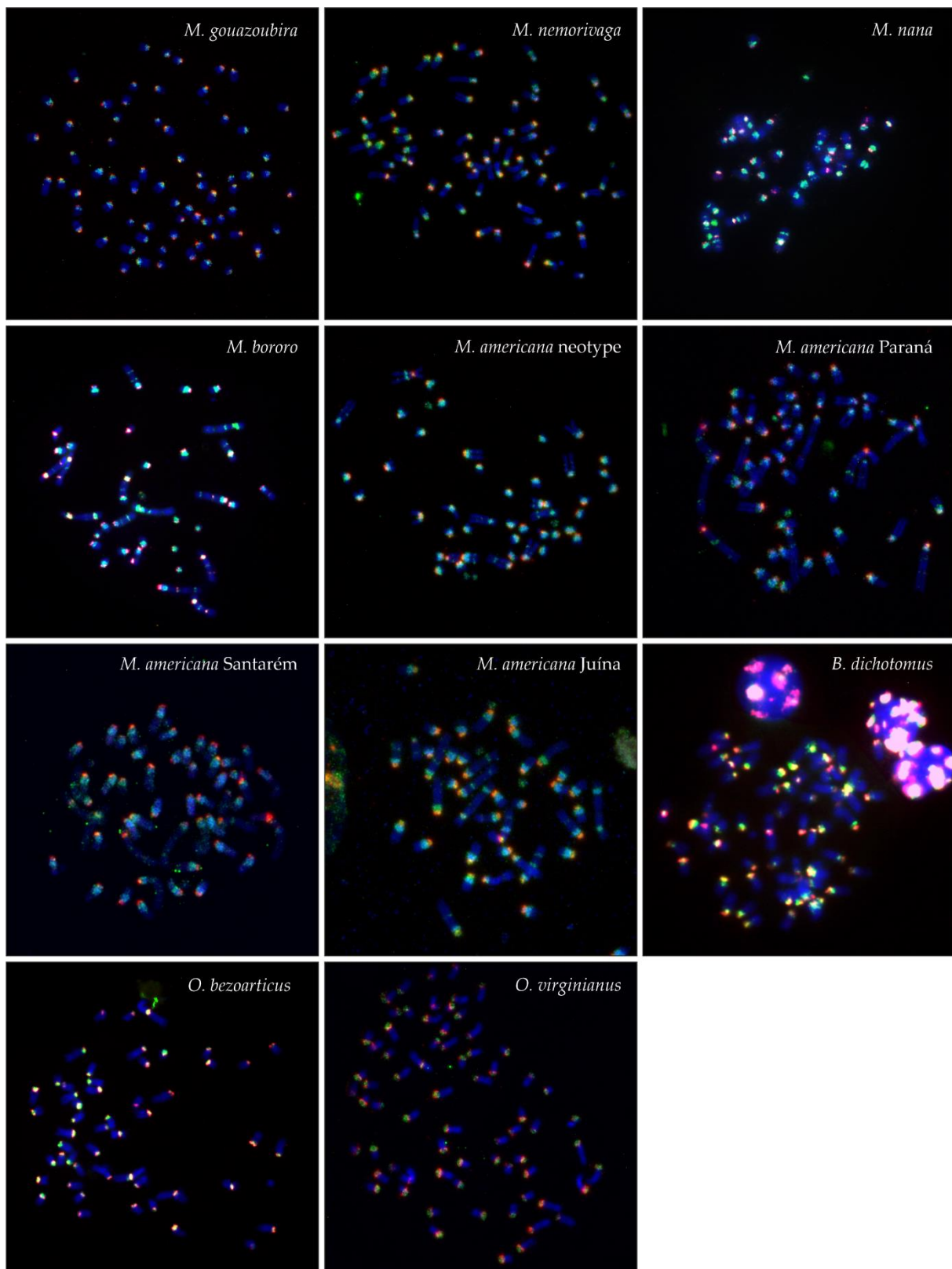


Figure 1. FISH patterns of the satI (green) and satII (red) DNA probe in the analyzed species.

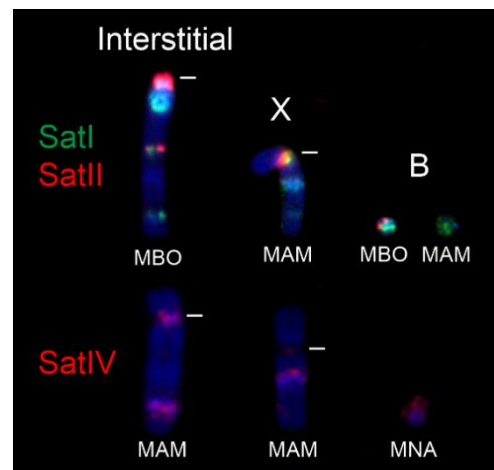


Figure 2. Examples of centromeric and interstitial satI, satII, and satIV signals on autosomes, X chromosomes, and B chromosomes. MBO—*M. bororo*, MNA—*M. nana*, MAM—*M. americana*. Centromeres are indicated by white lines.

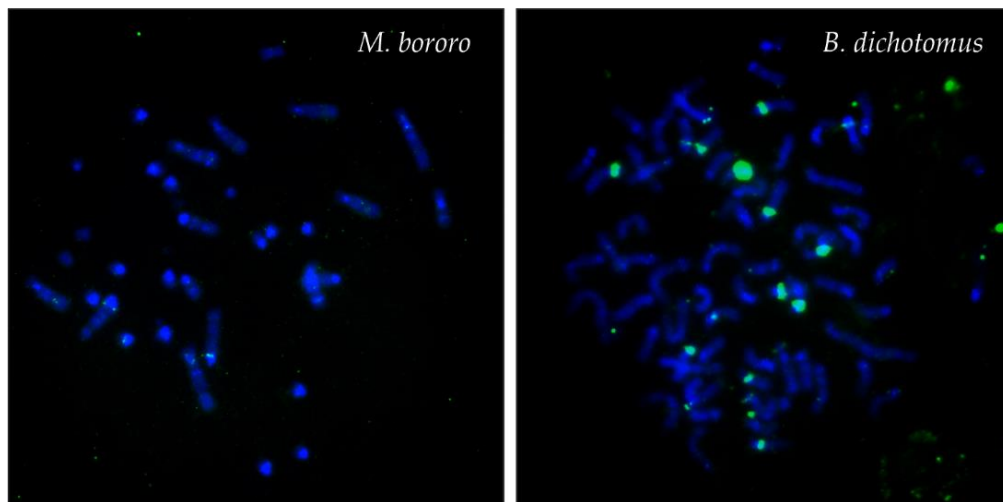


Figure 3. Examples of FISH patterns of the satIII (green) DNA probe in selected species. FISH pattern similar to the results in *M. bororo* was observed in all species except *B. dichotomus*.

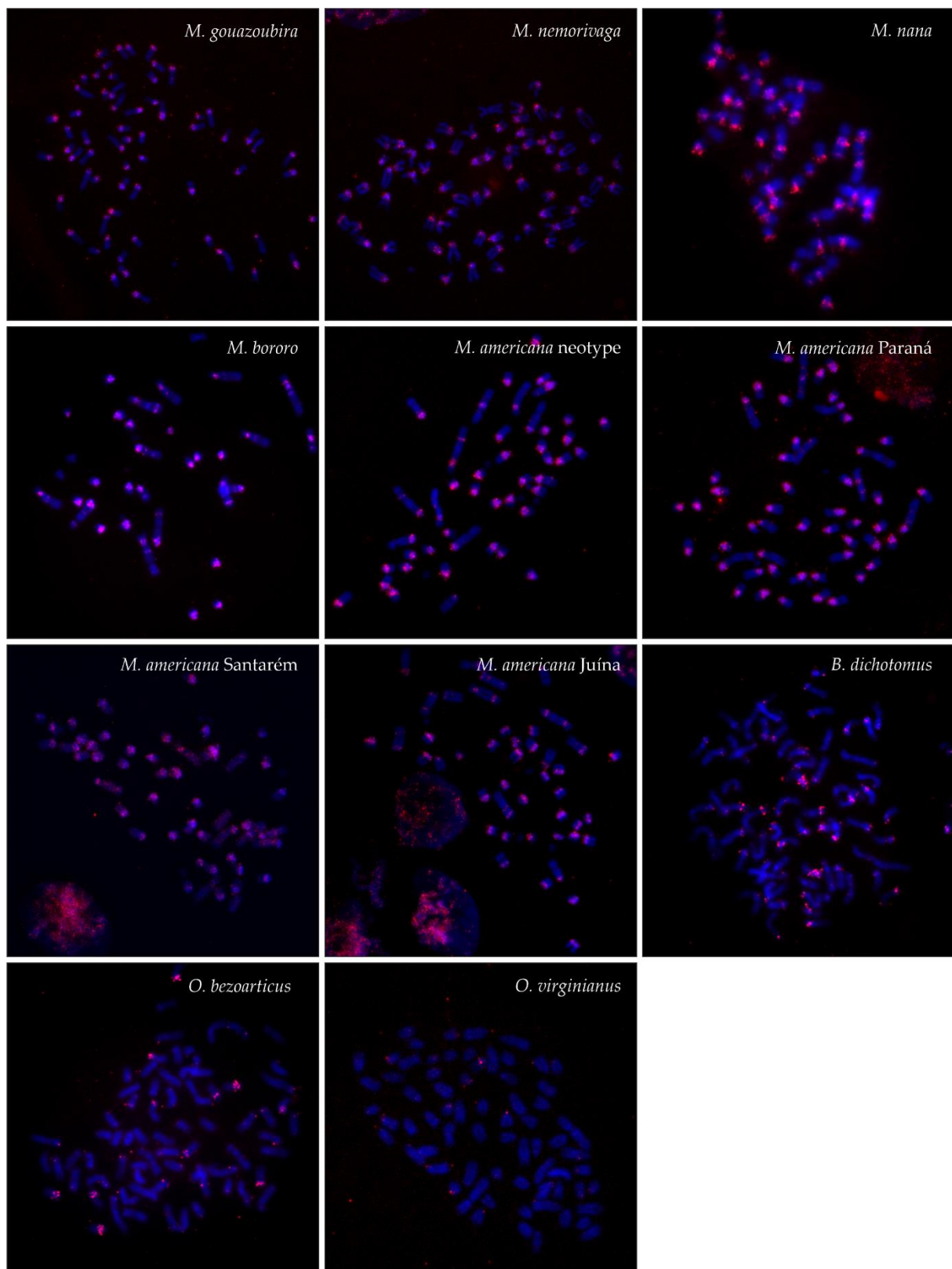


Figure 4. FISH patterns of the satIV (red) DNA probe in the analyzed species.

3.3. Phylogenetic Analysis

Together with previously published sequences, multiple sequence alignments consisted of 64 to 76 satI-IV sequences and 18 *mt-cyb* sequences of species from the family Cervidae (Table S4). The smart model selection algorithm suggested the GTR substitution model for the satI and satIII alignments, K80 model for the satII, and HKY model for the satIV and *mt-cyb* alignments. In all satDNA alignments, rate heterogeneity between sites was modelled according to the Γ distribution, and in the *mt-cyb* according to the proportion of invariable sites (Table S4). The satII and satIV phylogenies differentiated currently recognized tribes, with satII sequencing supporting monophyletic groups of Cervini, Muntiacini, Alceini, Capreolini, and Rangiferini (Figures 5B and 6B).

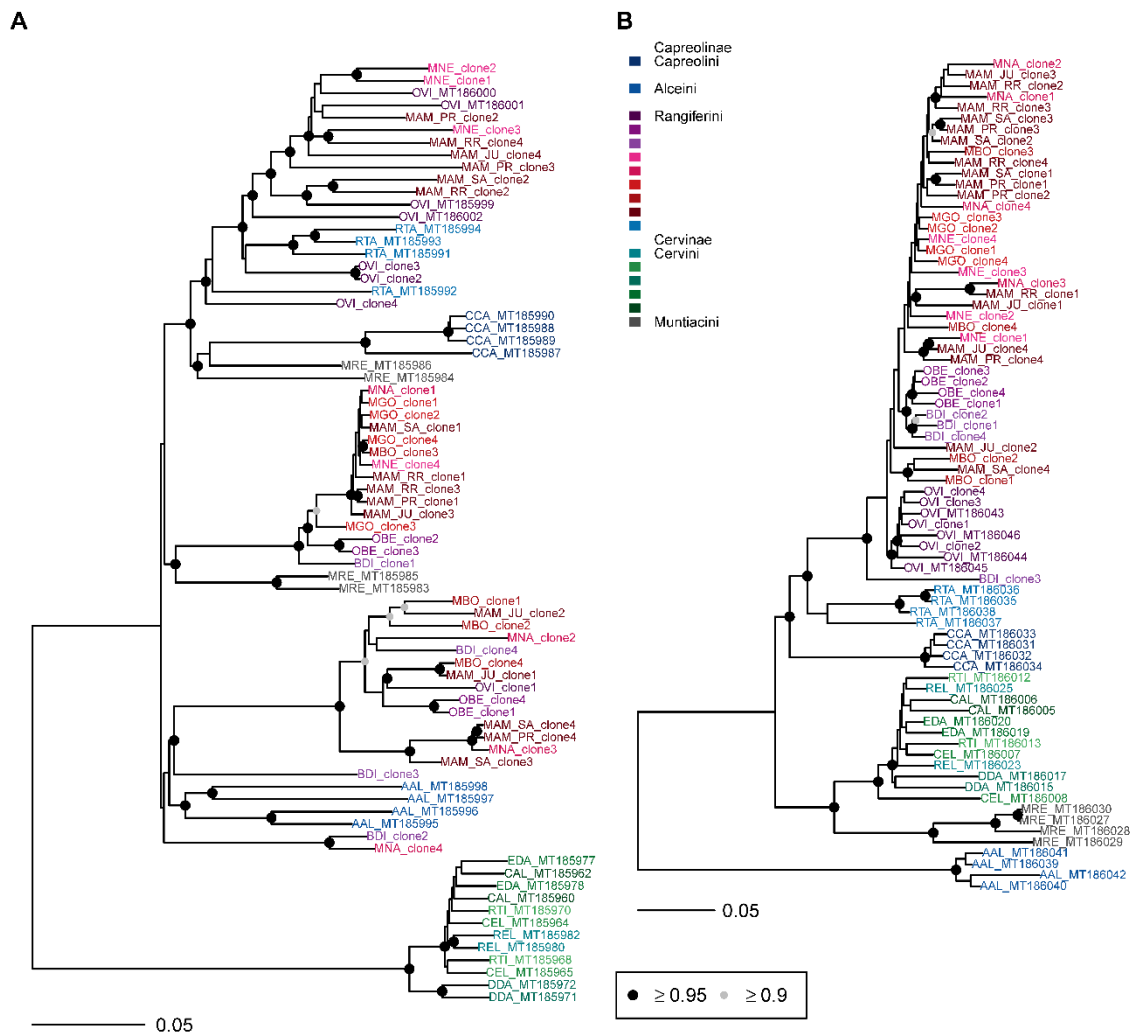


Figure 5. Bayesian phylogenetic trees constructed from cervid satellite sequences. (A) SatI, (B) satII. AAL—*Alces alces*, BDI—*Blastoceros dichotomus*, CAL—*Cervus albirostris*, CCA—*Capreolus capreolus*, CEL—*Cervus elaphus*, DDA—*Dama dama*, EDA—*Elaphurus davidianus*, MAM—*Mazama americana*, MBO—*Mazama bororo*, MGO—*Mazama gouazoubira*, MNA—*Mazama nana*, MNE—*Mazama nemorivaga*, MRE—*Muntiacus reevesi*, OBE—*Ozotoceros bezoarticus*, OVI—*Odocoileus virginianus*, REL—*Rucervus eldii*, RTA—*Rangifer tarandus*, RTI—*Rusa timorensis*. Circles at nodes signify nodes with posterior probability ≥ 0.95 (black) and ≥ 0.90 (grey). Unmarked nodes were not supported.

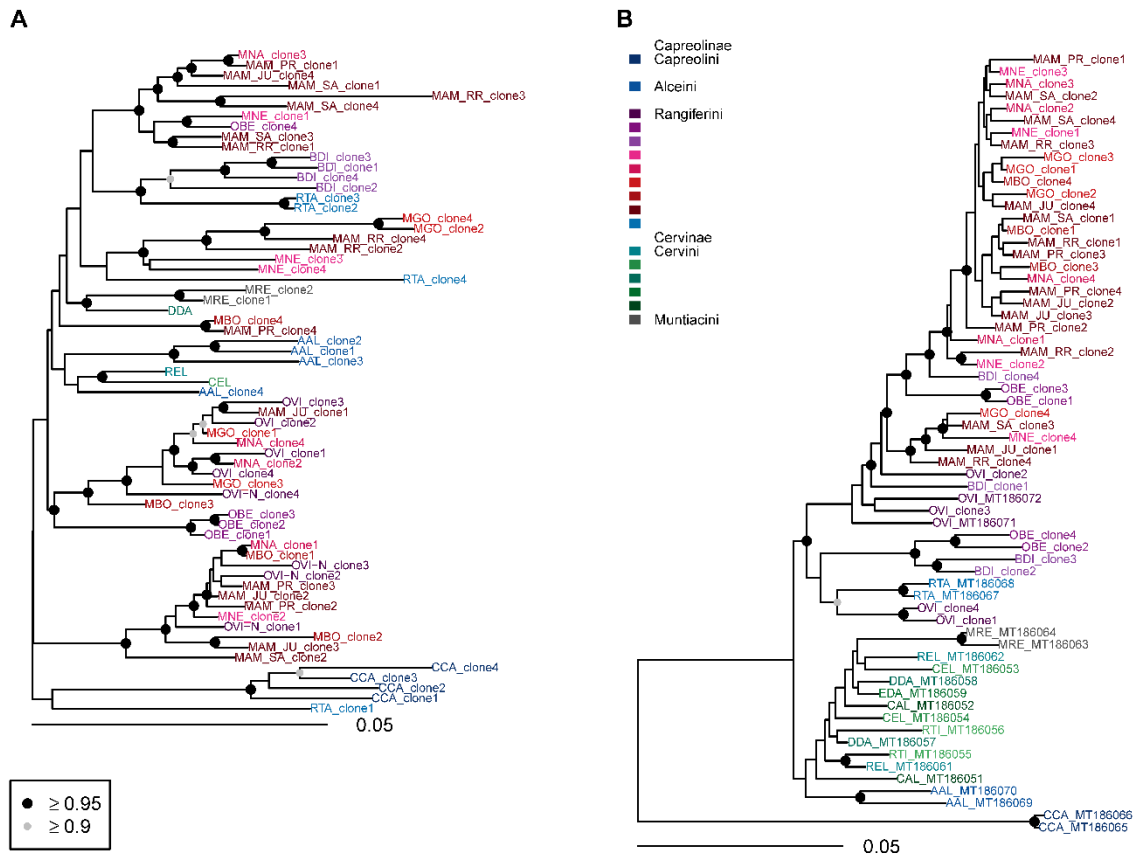


Figure 6. Bayesian phylogenetic trees constructed from cervid satellite sequences. (A) SatIII, (B) satIV. AAL—*Alces alces*, BDI—*Blastocerus dichotomus*, CAL—*Cervus albirostris*, CCA—*Capreolus capreolus*, CEL—*Cervus elaphus*, DDA—*Dama dama*, EDA—*Elaphurus davidianus*, MAM—*Mazama americana*, MBO—*Mazama bororo*, MGO—*Mazama gouazoubira*, MNA—*Mazama nana*, MNE—*Mazama nemorivaga*, MRE—*Muntiacus reevesi*, OBE—*Ozotoceros bezoarticus*, OVI—*Odocoileus virginianus*, REL—*Rucervus eldii*, RTA—*Rangifer tarandus*, RTI—*Rusa timorensis*. Circles at nodes signify nodes with posterior probability ≥ 0.95 (black) and ≥ 0.90 (grey). Unmarked nodes were not supported.

In satI phylogeny, a monophyletic relationship of satellite sequences was supported for Cervini, Alceini, and Capreolini, however Rangiferini and Muntiacini were polyphyletic (Figure 5A). The Neotropical deer satI sequences were diverged and formed three deeply differentiated lineages (Figure 6A). Clones from multiple species (*M. americana*, *M. nemorivaga*, *M. bororo*, *M. nana*, *O. bezoarticus*, *B. dichotomus*) were represented in more than one lineage. In *M. americana*, clones from all sampled regions were present in all three lineages. The first lineage included *Mazama*, *Odocoileus* (both populations), and Holarctic *Rangifer* in incomplete sorting of sequences at the species level, and the lineage formed a sister relationship to *Capreolus* and *Muntiacus*. The second Neotropical deer satI lineage consisted of *Mazama*, *Ozotoceros*, and *Blastocerus* as a sister group to two *Muntiacus* satI sequences. SatI clones from *M. gouazoubira* all belonged to the second lineage. The genera of Neotropical deer grouping in the third satI lineage were also *Mazama*, *Ozotoceros*, and *Blastocerus*, but no clear sister relationship was identified in the satI phylogeny (Figure 6A).

Neotropical deer formed a single supported lineage in the satII sequences with supported monophyly of *Odocoileus*, *Ozotoceros*, and *Blastocerus* (Figure 6B). The latter two taxa formed a paraphyletic sister relationship with respect to *Mazama*. Notably, BDI_clone3 formed a long branch at the base of Neotropical Rangiferini. Similar relationships were retrieved in the satIV phylogeny, but additional clones from all Neotropical genera grouped within the *Mazama* lineage (Figure 6B).

Low divergence in satIII-part (Table 3) resulted in incomplete lineage sorting in Neotropical deer and a polytomy at the deep divergence of Cervidae (Figure 6A).

The *mt-cyb* phylogeny showed monophyletic groups representing the tribes Rangiferini and Cervini (Figure S1). Muntiacini were sister to Cervini, and Capreolini and Alceini diverged rapidly close to the root of the tree. In Neotropical deer, mtDNA phylogeny did not support monophyly of *Mazama* similarly as was shown in the satDNA trees. Instead, *Mazama* were paraphyletic, with *M. nana*, *M. bororo*, and *M. americana* forming a single lineage sister to *O. virginianus*, and *M. gouazoubira* and *M. nemorivaga* forming an unresolved group with *B. dichotomus* and *O. bezoarticus* (Figure S1).

4. Discussion

Sequence Comparisons

Cervidae is a diverse group of species distributed in Eurasia and North and South America. Among them, Neotropical deer species have still been understudied in terms of current taxonomy and phylogenetic relationships [49]. In this study, we performed a comparative sequence and FISH analysis of the four main cervid satellite DNA families (satI-IV) isolated from a variety of Neotropical deer species, including several specific cytotypes.

Our sequence comparisons revealed close relationships among the studied Neotropical deer in satII, satIII and satIV DNA that also showed a high similarity to satellite DNA sequences available in the NCBI database for other species of Capreolinae. Regarding satI DNA, it showed the highest intra- and interspecific variability indicating a fast satI sequence evolution at the time of early divergence of the Capreolinae subfamily. The satI and satII monomer lengths were comparable to previously studied Capreolinae [24]. However, the number of the 31-bp satI internal subrepeat units was lower in the studied Neotropical deer than in other Capreolinae, and closer to that published in Cervini [24]. The general occurrence of this subrepeat throughout many bovid and cervid genomes [21, 24,28,50] indicates its possible biological function. This suggestion is also supported by the interspecies similarity in the 31-bp subrepeat sequences at the individual positions of the satI DNA monomers. This sequence might form a part of a 3D structure involved in protein or siRNA binding during heterochromatin formation, cell division, or transcription regulation. However, further studies are needed to elucidate its functions.

The highest GC content and the presence of the CENP-B binding motif, known to be associated with the centromeric function [51,52], were detected in the satII DNA in all studied Neotropical deer. These findings support the previously published hypothesis that satII DNA might represent the most important satellite DNA family in Cervidae [24] but the satII DNA significance has yet to be confirmed by functional studies. The sequence of the 17-bp CENP-B motif was identical throughout most analyzed Neotropical deer samples indicating a high level of conservation. The most common CENP-B motif sequence detected in this study (TTTGGAGGCAGGCGGG) contained the published human core recognition sequence (NTTCGNNNNANNCGGN) [53] with one nucleotide difference (C-G substitution). However, three different one-nucleotide substitutions from the deer core sequence were revealed in *M. bororo*, indicating a surprising CENP-B motif variance in this species that probably originated during its separate evolution.

In Cervidae, satI and satII DNA sequences are highly abundant, occupying 2–35% of the genomic DNA [33]. On the other hand, low copy numbers of satIII and satIV DNA not detectable by FISH were previously reported in many deer species [24]. In this study, we also observed significant differences in the abundance of the satellite DNA families by FISH. The high copy numbers of satI and satII DNA, reflected by large hybridization signals, were in contrast to very weak satIII signals only present on one or a few chromosomes in all studied species except *B. dichotomus*. Regarding satIV DNA, there were significant differences in its abundance between *O. virginianus*, *B. dichotomus* and *O. bezoarticus* on one side, and species of the genus *Mazama* on the other, the latter showing large satIV DNA blocks. The observed interspecies differences in the satellite DNA abundance at the relatively high sequence similarity of the repeat units can be related to the satellite DNA evolution. It is generally accepted that satellite DNAs are formed by a fast amplification of

monomers existing in ancestral genomes [54]. As suggested by a library model, related species share a common collection of satellite DNAs, which vary in their abundance, with specific sequences being differentially amplified in individual species [55–57]. Satellite DNA arrays are probably formed by a mechanism of rolling circle replication with subsequent further amplification by unequal crossing over [58–61]. The existing sequences are then diversified by mutations, which spread through the genome by mechanisms of concerted evolution, leading to the formation of species- and chromosome-specific satellite sequences [13,62–64]. Accordingly, interspecies differences in satellite DNA abundance and sequences were found to be highly consistent with species phylogeny [16,22,24,56,63,65].

In this study, the satII DNA sequence phylogeny well corresponds to the mtDNA (*mt-cyb* gene) phylogeny (Figure S1) and the published taxonomic divergences in Cervidae [24]. The satII phylogeny differentiated the currently recognized tribes, suggesting monophyletic origin of Cervini, Muntiacini, Alceini, Capreolini, and Rangiferini. In Neotropical deer, *O. bezoarticus* was closely related to *B. dichotomus*, and both Neotropical and Nearctic populations of *O. virginianus* formed one lineage without defined intraspecific relationships. SatII and satIV sequences of *Mazama* showed unresolved relationships both at the level of species differentiation as well as at the genus level. Incomplete lineage sorting of *Mazama* species with respect to other Neotropical deer consistently occurs in satellite DNA (this study), mtDNA phylogenies (Figure S1 and [66,67]), and even with the molecular and morphological data combined [68]. Neotropical deer, as descendants of Nearctic ancestors that arrived to South America during the Great America Biotic Interchange between late Miocene and late Pleistocene [69], diverged in an explosive radiation, forming morphologically well-defined but genetically unresolved genera. As in other Neotropical mammals, morphological convergence in genetically diverged taxa could be attributed to ecological adaptations to specific niche partitioning in newly colonized regions [70,71]. In this study, the explosive radiation in Neotropical deer can be best observed in the satI sequence phylogeny. At least four distinct lineages first began to diverge at the time of the split of Capreolinae. Genera *Rangifer*, *Capreolus*, and *Alces* each retained one lineage of satI sequences, but in Neotropical deer, satI sequences diversified three times independently.

The presence of genomic satellite DNA arrays can facilitate the formation of chromosome rearrangements and thus karyotype and species evolution [29,72,73]. The deer chromosome evolution from the ancestral karyotype ($2n = 70$) was driven by centric and tandem fusions at the simultaneous reduction in the chromosome number [9]. Moreover, the existence of centric fusion polymorphisms previously described in the genus *Mazama* indicate that chromosome fusions represent an important source of the recent and ongoing karyotype evolution of this taxon [74–76]. Despite the predominantly peri/centromeric location of the satellite DNA, we also observed interstitial satI, satII, and satIV FISH signals in *Mazama* species with highly reduced chromosome numbers (*M. nana*, *M. bororo*, *M. americana* cytotypes). Similar finding of interstitial satellite DNA signals at the tandem fusion sites, and even their co-localization with telomeric sequences was previously reported in muntjacs [30,32,77–79].

In *M. americana*, a multiple sexual system resulting from evolutionary X-autosomal fusions was previously described [12,80]. Among deer, the XY1Y2 system was found also in the genus *Muntiacus* [81,82]. It is known that sex-autosomal translocations are usually associated with a disturbed process of X chromosome inactivation and with a meiotic disruption [83–85]. However, heterochromatin blocks intercalated between the gonosomal and autosomal parts of the rearranged sex-autosomes can serve as effective barriers for spreading of somatic X-chromosome inactivation in females and for regulation of meiotic processes in males [86–88]. In our study, the presence of intercalated heterochromatin in the X-autosomal fusion region suggested by a distinct DAPI band was proved by detection of satI, less frequently satII and satIV hybridisation signals in all *M. americana* cytotypes. As discussed in the previous paragraph, also these interstitial satellite DNA signals probably map to a historical fusion site and represent former centromeric heterochromatin of the autosome fused to the ancestral X chromosome.

Another interesting karyotype feature of *Mazama* species analyzed in this study is the presence of B chromosomes [7,12,75,80]. B chromosomes are supernumerary, mitotically unstable chromosomes that were described in some animal, plant, and fungal species [89]. Their numbers vary in different individuals and even individual cells of the organism, and, despite a presence of duplicated coding genes detected in Bs in some species [90,91], their biological function is unknown. A recent study based on comparative FISH and next-generation sequencing of B chromosomes in two deer species, *Capreolus pygargus* (Capreolini) and *M. gouazoubira* (Rangiferini) demonstrated an independent origin of B chromosomes in these species, and their different evolutionary history [92]. In all animals carrying B chromosomes in our study, the Bs showed FISH signals of the satI DNA probe. The independent divergent lineages observed in Neotropical deer in the satI phylogeny might be attributed to satI sequences on the B chromosomes. Moreover, the satII DNA signals were detected on Bs in *M. bororo*. This might indicate either an independent origin or a more primitive stage of the B chromosomes in *M. bororo*, which have not yet led to an evolutionary satII DNA sequence degeneration in this species.

5. Conclusions

The Neotropical deer species show high intra- and interspecies satellite DNA sequence similarities indicating close evolutionary relationships. The high satellite DNA abundance probably stands behind the cervid karyotype differentiation driven by centric and tandem fusions at the simultaneous reduction of the chromosome number.

Supplementary Materials: The following are available online at <https://www.mdpi.com/2073-4425/12/1/123/s1>: Table S1. Primers and annealing temperatures for satellite DNA isolation. Table S2. Positions and sequences of the CENP-B binding motif in individual satII DNA clones. Table S3. The 31-bp subrepeat sequence variance and its positions in the satI DNA sequence. Table S4. Multiple sequence alignment composition and selected substitution models of cervid satellite and mitochondrial sequences. Figure S1. Bayesian phylogenetic tree constructed from cervid *mt-cyb* sequences. AAL—*Alces alces*, BDI—*Blastocercus dichotomus*, CAL—*Cervus albirostris*, CCA—*Capreolus capreolus*, CEL—*Cervus elaphus*, DDA—*Dama dama*, EDA—*Elaphurus davidianus*, MAM—*Mazama americana*, MBO—*Mazama bororo*, MGO—*Mazama gouazoubira*, MNA—*Mazama nana*, MNE—*Mazama nemorivaga*, MRE—*Muntiacus reevesi*, OBE—*Ozotoceros bezoarticus*, OVI—*Odocoileus virginianus*, REL—*Rucervus eldii*, RTA—*Rangifer tarandus*, RTI—*Rusa timorensis*. Circles at nodes signify nodes with posterior probability ≥ 0.95 (black) and ≥ 0.90 (grey). Unmarked nodes were not supported.

Author Contributions: Conceptualization, S.K., M.V. and J.R.; investigation, M.V., S.K., N.M., A.M.B., D.J.G., H.C., D.K. and P.M.; methodology, M.V. and S.K. and N.M.; supervision, J.R. and J.M.D.; writing—original draft, M.V., S.K. and N.M.; writing—review and editing, D.J.G., J.M.D. and J.R. All authors have read and agreed to the published version of the manuscript.

Funding: This research was funded by the Czech Science Foundation grant number 20-22517J, the São Paulo Research Foundation FAPESP 2019/06940-1-GACR, FONDECYT grant No. 116-2017, Ministry of Agriculture of the Czech Republic, grant No. RO 0520, and Ministry of Education, Youth and Sports of the Czech Republic under the project CEITEC 2020, grant No. LQ1601.

Institutional Review Board Statement: The study was conducted according to the guidelines of the Declaration of Helsinki, and approved by the Ethics Committee on Animal Use of the School of Agricultural and Veterinarian Sciences, São Paulo State University (protocol code 005433/19).

Informed Consent Statement: Not applicable.

Data Availability Statement: The data presented in this study are available in the article and supplementary material.

Acknowledgments: The authors wish to thank to the whole NUPECCE team for their collaborative support.

Conflicts of Interest: The authors declare no conflict of interest. The funders had no role in the design of the study; in the collection, analyses, or interpretation of data; in the writing of the manuscript, or in the decision to publish the results.

Ethical Statement: The biological material for tissue culture was obtained by a veterinarian during medical examination of the animals. All procedures performed in this study were in accordance with the ethical standards of the Veterinary Research Institute (Brno, Czech Republic), which complies with the Czech and European Union Legislation for the protection of animals used for scientific purposes.

References

- Wilson, D.E.; Reeder, D.M. *Mammal Species of the World: A Taxonomic and Geographic Reference*; Johns Hopkins University Press: Baltimore, MD, USA, 2005; ISBN 978-0-8018-8221-0.
- Chen, L.; Qiu, Q.; Jiang, Y.; Wang, K.; Lin, Z.; Li, Z.; Bibi, F.; Yang, Y.; Wang, J.; Nie, W.; et al. Large-Scale Ruminant Genome Sequencing Provides Insights into Their Evolution and Distinct Traits. *Science* **2019**, *364*. [[CrossRef](#)] [[PubMed](#)]
- Gutiérrez, E.E.; Helgen, K.M.; McDonough, M.M.; Bauer, F.; Hawkins, M.T.R.; Escobedo-Morales, L.A.; Patterson, B.D.; Maldonado, J.E. A Gene-Tree Test of the Traditional Taxonomy of American Deer: The Importance of Voucher Specimens, Geographic Data, and Dense Sampling. *ZooKeys* **2017**, *697*, 87–131. [[CrossRef](#)]
- Duarte, J.M.B.; González, S.; Maldonado, J.E. The Surprising Evolutionary History of South American Deer. *Mol. Phylogenet. Evol.* **2008**, *49*, 17–22. [[CrossRef](#)] [[PubMed](#)]
- Groves, C.; Grubb, P. *Ungulate Taxonomy*, 1st ed.; Johns Hopkins University Press: Baltimore, MD, USA, 2011; ISBN 978-1-4214-0093-8.
- Fontana, F.; Rubini, M. Chromosomal Evolution in Cervidae. *BioSystems* **1990**, *24*, 157–174. [[CrossRef](#)]
- Duarte, J.M.B.; Jorge, W. Morphologic and Cytogenetic Description of the Small Red Brocket (Mazama Bororo Duarte, 1996) in Brazil. *Mammalia* **2009**, *67*, 403–410. [[CrossRef](#)]
- Huang, L.; Chi, J.; Nie, W.; Wang, J.; Yang, F. Phylogenomics of Several Deer Species Revealed by Comparative Chromosome Painting with Chinese Muntjac Paints. *Genetica* **2006**, *127*, 25–33. [[CrossRef](#)] [[PubMed](#)]
- Nietzel, H. Chromosome Evolution of Cervidae: Karyotypic and Molecular Aspects. In *Cytogenetics: Basic and Applied Aspects*; Obe, G., Basler, A., Eds.; Springer: Berlin/Heidelberg, Germany, 1987; ISBN 978-3-642-72804-4.
- Cifuentes-Rincón, A.; Morales-Donoso, J.A.; Sandoval, E.D.P.; Tomazella, I.M.; Mantelatto, A.M.B.; de Thoisy, B.; Duarte, J.M.B. Designation of a Neotype for Mazama Americana (Artiodactyla, Cervidae) Reveals a Cryptic New Complex of Brocket Deer Species. *ZooKeys* **2020**, *958*, 143–164. [[CrossRef](#)]
- Cursino, M.S.; Salviano, M.B.; Abril, V.V.; Zanetti, E.; dos, S.; Duarte, J.M. The Role of Chromosome Variation in the Speciation of the Red Brocket Deer Complex: The Study of Reproductive Isolation in Females. *BMC Evol. Biol.* **2014**, *14*, 40. [[CrossRef](#)]
- Abril, V.V.; Carnelossi, E.A.G.; González, S.; Duarte, J.M.B. Elucidating the Evolution of the Red Brocket Deer Mazama Americana Complex (Artiodactyla; Cervidae). *Cytogenet. Genome Res.* **2010**, *128*, 177–187. [[CrossRef](#)]
- Plohl, M.; Luchetti, A.; Mestrovic, N.; Mantovani, B. Satellite DNAs between Selfishness and Functionality: Structure, Genomics and Evolution of Tandem Repeats in Centromeric (Hetero)Chromatin. *Gene* **2008**, *409*, 72–82. [[CrossRef](#)]
- Ugarković, D.; Plohl, M. Variation in Satellite DNA Profiles—Causes and Effects. *EMBO J.* **2002**, *21*, 5955–5959. [[CrossRef](#)] [[PubMed](#)]
- Schalch, T.; Steiner, F.A. Structure of Centromere Chromatin: From Nucleosome to Chromosomal Architecture. *Chromosoma* **2017**, *126*, 443–455. [[CrossRef](#)] [[PubMed](#)]
- Kunze, B.; Traut, W.; Garagna, S.; Weichenhan, D.; Redi, C.A.; Winking, H. Pericentric Satellite DNA and Molecular Phylogeny in *Acomys* (Rodentia). *Chromosome Res.* **1999**, *7*, 131. [[CrossRef](#)] [[PubMed](#)]
- Louzada, S.; Vieira-da-Silva, A.; Mendes-da-Silva, A.; Kubickova, S.; Rubes, J.; Adegá, F.; Chaves, R. A Novel Satellite DNA Sequence in the *Peromyscus* Genome (PMSat): Evolution via Copy Number Fluctuation. *Mol. Phylogenet. Evol.* **2015**, *92*, 193–203. [[CrossRef](#)] [[PubMed](#)]
- Baicharoen, S.; Miyabe-Nishiwaki, T.; Arsaithamkul, V.; Hirai, Y.; Duangsa-ard, K.; Siriaroonrat, B.; Domae, H.; Srikulnath, K.; Koga, A.; Hirai, H. Locational Diversity of Alpha Satellite DNA and Intergeneric Hybridization Aspects in the *Nomascus* and *Hylobates* Genera of Small Apes. *PLoS ONE* **2014**, *9*, e109151. [[CrossRef](#)]
- Vozdova, M.; Kubickova, S.; Cernohorska, H.; Fröhlich, J.; Vodicka, R.; Rubes, J. Comparative Study of the Bush Dog (*Speothos venaticus*) Karyotype and Analysis of Satellite DNA Sequences and Their Chromosome Distribution in Six Species of Canidae. *Cytogenet. Genome Res.* **2019**, *159*, 88–96. [[CrossRef](#)] [[PubMed](#)]
- Vozdova, M.; Kubickova, S.; Cernohorska, H.; Fröhlich, J.; Rubes, J. Satellite DNA Sequences in Canidae and Their Chromosome Distribution in Dog and Red Fox. *Cytogenet. Genome Res.* **2016**, *150*, 118–127. [[CrossRef](#)]
- Jobse, C.; Buntjer, J.B.; Haagsma, N.; Breukelman, H.J.; Beintema, J.J.; Lenstra, J.A. Evolution and Recombination of Bovine DNA Repeats. *J. Mol. Evol.* **1995**, *41*, 277–283. [[CrossRef](#)]
- Kopečna, O.; Kubickova, S.; Cernohorska, H.; Cabelova, K.; Vahala, J.; Martinkova, N.; Rubes, J. Tribe-Specific Satellite DNA in Non-Domestic Bovidae. *Chromosome Res.* **2014**, *22*, 277–291. [[CrossRef](#)]
- Chaves, R.; Guedes-Pinto, H.; Heslop-Harrison, J.S. Phylogenetic Relationships and the Primitive X Chromosome Inferred from Chromosomal and Satellite DNA Analysis in Bovidae. *Proc. Biol. Sci.* **2005**, *272*, 2009–2016. [[CrossRef](#)]
- Vozdova, M.; Kubickova, S.; Cernohorska, H.; Fröhlich, J.; Martinková, N.; Rubes, J. Sequence Analysis and FISH Mapping of Four Satellite DNA Families among Cervidae. *Genes* **2020**, *11*, 584. [[CrossRef](#)] [[PubMed](#)]

25. Slamovits, H.C.; Cook, J.A.; Lessa, E.P.; Rossi, M.S. Recurrent Amplifications and Deletions of Satellite DNA Accompanied Chromosomal Diversification in South American Tuco-Tucos (Genus *Ctenomys*, Rodentia: Octodontidae): A Phylogenetic Approach. *Mol. Biol. Evol.* **2001**, *18*, 1708–1719. [[CrossRef](#)] [[PubMed](#)]
26. Bachmann, L.; Sperlich, D. Gradual Evolution of a Specific Satellite DNA Family in *Drosophila Ambigua*, *D. Tristis*, and *D. Obscura*. *Mol. Biol. Evol.* **1993**, *10*, 647–659. [[PubMed](#)]
27. Garrido-Ramos, M.A.; de la Herrán, R.; Jamilena, M.; Lozano, R.; Ruiz Rejón, C.; Ruiz Rejón, M. Evolution of Centromeric Satellite DNA and Its Use in Phylogenetic Studies of the Sparidae Family (Pisces, Perciformes). *Mol. Phylogenet. Evol.* **1999**, *12*, 200–204. [[CrossRef](#)]
28. Lee, C.; Court, D.R.; Cho, C.; Haslett, J.L.; Lin, C.C. Higher-Order Organization of Subrepeats and the Evolution of Cervid Satellite DNA. *J. Mol. Evol.* **1997**, *44*, 327–335. [[CrossRef](#)]
29. Li, Y.-C.; Lin, C.-C. Cervid Satellite DNA and Karyotypic Evolution of Indian Muntjac. *Genes Genom.* **2012**, *34*, 7–11. [[CrossRef](#)]
30. Liu, Y.; Nie, W.; Huang, L.; Wang, J.; Su, W.; Lin, C.; Yang, F. Cloning, Characterization, and FISH Mapping of Four Satellite DNAs from Black Muntjac (*Muntiacus crinifrons*) and Fea's Muntjac (*M. feae*). *Zool. Res.* **2008**, *2008*, 225–235. [[CrossRef](#)]
31. Lin, C.C.; Li, Y.C. Chromosomal Distribution and Organization of Three Cervid Satellite DNAs in Chinese Water Deer (*Hydropotes inermis*). *Cytogenet. Genome Res.* **2006**, *114*, 147–154. [[CrossRef](#)]
32. Li, Y.C.; Lee, C.; Chang, W.S.; Li, S.-Y.; Lin, C.C. Isolation and Identification of a Novel Satellite DNA Family Highly Conserved in Several Cervidae Species. *Chromosoma* **2002**, *111*, 176–183. [[CrossRef](#)]
33. Blake, R.D.; Wang, J.Z.; Beaugregard, L. Repetitive Sequence Families in *Alces Alces Americana*. *J. Mol. Evol.* **1997**, *44*, 509–520. [[CrossRef](#)]
34. Li, Y.C.; Lee, C.; Hseu, T.H.; Li, S.Y.; Lin, C.C.; Hsu, T.H. Direct Visualization of the Genomic Distribution and Organization of Two Cervid Centromeric Satellite DNA Families. *Cytogenet. Cell Genet.* **2000**, *89*, 192–198. [[CrossRef](#)]
35. Phucienniczak, A.; Skowroński, J.; Jaworski, J. Nucleotide Sequence of Bovine 1.715 Satellite DNA and Its Relation to Other Bovine Satellite Sequences. *J. Mol. Biol.* **1982**, *158*, 293–304. [[CrossRef](#)]
36. Masumoto, H.; Masukata, H.; Muro, Y.; Nozaki, N.; Okazaki, T. A Human Centromere Antigen (CENP-B) Interacts with a Short Specific Sequence in Alphoid DNA, a Human Centromeric Satellite. *J. Cell Biol.* **1989**, *109*, 1963–1973. [[CrossRef](#)] [[PubMed](#)]
37. Grant, C.E.; Bailey, T.L.; Noble, W.S. FIMO: Scanning for Occurrences of a given Motif. *Bioinformatics* **2011**, *27*, 1017–1018. [[CrossRef](#)] [[PubMed](#)]
38. Katoh, K.; Rozewicki, J.; Yamada, D.K. MAFFT Online Service: Multiple Sequence Alignment, Interactive Sequence Choice and Visualization. *Brief. Bioinform.* **2019**, *20*, 1160–1166. [[CrossRef](#)] [[PubMed](#)]
39. Katoh, K.; Kuma, K.; Toh, H.; Miyata, T. MAFFT Version 5: Improvement in Accuracy of Multiple Sequence Alignment. *Nucleic Acids Res.* **2005**, *33*, 511–518. [[CrossRef](#)]
40. Machado, D.J.; Castroviejo-Fisher, S.; Grant, T. Evidence of Absence Treated as Absence of Evidence: The Effects of Variation in the Number and Distribution of Gaps Treated as Missing Data on the Results of Standard Maximum Likelihood Analysis. *Mol. Phylogenet. Evol.* **2021**, *154*, 106966. [[CrossRef](#)] [[PubMed](#)]
41. Lefort, V.; Longueville, J.-E.; Gascuel, O. SMS: Smart Model Selection in PhyML. *Mol. Biol. Evol.* **2017**, *34*, 2422–2424. [[CrossRef](#)] [[PubMed](#)]
42. Guindon, S.; Dufayard, J.-F.; Lefort, V.; Anisimova, M.; Hordijk, W.; Gascuel, O. New Algorithms and Methods to Estimate Maximum-Likelihood Phylogenies: Assessing the Performance of PhyML 3. *Syst. Biol.* **2010**, *59*, 307–321. [[CrossRef](#)] [[PubMed](#)]
43. Ronquist, F.; Teslenko, M.; van der Mark, P.; Ayres, D.L.; Darling, A.; Höhna, S.; Larget, B.; Liu, L.; Suchard, M.A.; Huelsenbeck, J.P. MrBayes 3.2: Efficient Bayesian Phylogenetic Inference and Model Choice across a Large Model Space. *Syst. Biol.* **2012**, *61*, 539–542. [[CrossRef](#)] [[PubMed](#)]
44. R Core Team. *R: A Language and Environment for Statistical Computing*; R Foundation for Statistical Computing: Vienna, Austria, 2020.
45. Paradis, E.; Schliep, K. Ape 5.0: An Environment for Modern Phylogenetics and Evolutionary Analyses in R. *Bioinformatics* **2019**, *35*, 526–528. [[CrossRef](#)]
46. Wang, L.-G.; Lam, T.T.-Y.; Xu, S.; Dai, Z.; Zhou, L.; Feng, T.; Guo, P.; Dunn, C.W.; Jones, B.R.; Bradley, T.; et al. Treeio: An R Package for Phylogenetic Tree Input and Output with Richly Annotated and Associated Data. *Mol. Biol. Evol.* **2020**, *37*, 599–603. [[CrossRef](#)]
47. Revell, L.J. Phytools: An R Package for Phylogenetic Comparative Biology (and Other Things). *Methods Ecol. Evol.* **2012**, *3*, 217–223. [[CrossRef](#)]
48. Neuwirth, E. RColorBrewer: ColorBrewer Palettes. 2014. Available online: <https://CRAN.R-project.org/package=RColorBrewer> (accessed on 7 December 2014).
49. Barbanti Duarte, J.M.; González, S. Neotropical Cervidology, Biology and Medicine of Latin American Deer. Available online: <https://www.iucn.org/content/neotropical-cervidology> (accessed on 23 November 2020).
50. Bogenberger, J.M.; Neumaier, P.S.; Fittler, F. The Muntjac Satellite IA Sequence Is Composed of 31-Base-Pair Internal Repeats That Are Highly Homologous to the 31-Base-Pair Subrepeats of the Bovine Satellite 1. *Eur. J. Biochem.* **1985**, *148*, 55–59. [[CrossRef](#)] [[PubMed](#)]
51. Vafa, O.; Shelby, R.D.; Sullivan, K.F. CENP-A Associated Complex Satellite DNA in the Kinetochores of the Indian Muntjac. *Chromosoma* **1999**, *108*, 367–374. [[CrossRef](#)] [[PubMed](#)]

52. Carroll, C.W.; Silva, M.C.C.; Godek, K.M.; Jansen, L.E.T.; Straight, A.F. Centromere Assembly Requires the Direct Recognition of CENP-A Nucleosomes by CENP-N. *Nat. Cell Biol.* **2009**, *11*, 896–902. [[CrossRef](#)] [[PubMed](#)]
53. Suntronpong, A.; Kugou, K.; Masumoto, H.; Srikulnath, K.; Ohshima, K.; Hirai, H.; Koga, A. CENP-B Box, a Nucleotide Motif Involved in Centromere Formation, Occurs in a New World Monkey. *Biol. Lett.* **2016**, *12*. [[CrossRef](#)] [[PubMed](#)]
54. Ruiz-Ruano, F.J.; López-León, M.D.; Cabrero, J.; Camacho, J.P.M. High-Throughput Analysis of the Satellitome Illuminates Satellite DNA Evolution. *Sci. Rep.* **2016**, *6*. [[CrossRef](#)] [[PubMed](#)]
55. Mestrovic, N.; Plohl, M.; Mravinac, B.; Ugarković, D. Evolution of Satellite DNAs from the Genus *Palorus*—Experimental Evidence for the “Library” Hypothesis. *Mol. Biol. Evol.* **1998**, *15*, 1062–1068. [[CrossRef](#)] [[PubMed](#)]
56. Palacios-Gimenez, O.M.; Milani, D.; Song, H.; Marti, D.A.; López-León, M.D.; Ruiz-Ruano, F.J.; Camacho, J.P.M.; Cabral-de-Mello, D.C. Eight Million Years of Satellite DNA Evolution in Grasshoppers of the Genus *Schistocerca* Illuminate the Ins and Outs of the Library Hypothesis. *Genome Biol. Evol.* **2020**, *12*, 88–102. [[CrossRef](#)]
57. Fry, K.; Salser, W. Nucleotide Sequences of HS- α Satellite DNA from Kangaroo Rat *Dipodomys Ordii* and Characterization of Similar Sequences in Other Rodents. *Cell* **1977**, *12*, 1069–1084. [[CrossRef](#)]
58. Walsh, J.B. Persistence of Tandem Arrays: Implications for Satellite and Simple-Sequence DNAs. *Genetics* **1987**, *115*, 553–567. [[CrossRef](#)] [[PubMed](#)]
59. Okumura, K.; Kiyama, R.; Oishi, M. Sequence Analyses of Extrachromosomal Sau3A and Related Family DNA: Analysis of Recombination in the Excision Event. *Nucleic Acids Res.* **1987**, *15*, 7477–7489. [[CrossRef](#)] [[PubMed](#)]
60. Alkan, C.; Eichler, E.E.; Bailey, J.A.; Sahinalp, S.C.; Tüzün, E. The Role of Unequal Crossover in Alpha-Satellite DNA Evolution: A Computational Analysis. *J. Comput. Biol.* **2004**, *11*, 933–944. [[CrossRef](#)] [[PubMed](#)]
61. Stephan, W. Recombination and the Evolution of Satellite DNA. *Genet. Res.* **1986**, *47*, 167–174. [[CrossRef](#)]
62. Dover, G.A. Molecular Drive in Multigene Families: How Biological Novelities Arise, Spread and Are Assimilated. *Trends Genet.* **1986**, *2*, 159–165. [[CrossRef](#)]
63. Lorite, P.; Muñoz-López, M.; Carrillo, J.A.; Sanlloriente, O.; Vela, J.; Mora, P.; Tinaut, A.; Torres, M.I.; Palomeque, T. Concerted Evolution, a Slow Process for Ant Satellite DNA: Study of the Satellite DNA in the *Aphaenogaster* Genus (Hymenoptera, Formicidae). *Org. Divers. Evol.* **2017**, *17*, 595–606. [[CrossRef](#)]
64. Durfy, S.J.; Willard, H.F. Concerted Evolution of Primate Alpha Satellite DNA: Evidence for an Ancestral Sequence Shared by Gorilla and Human X Chromosome Alpha Satellite. *J. Mol. Biol.* **1990**, *216*, 555–566. [[CrossRef](#)]
65. Mravinac, B.; Plohl, M. Parallelism in Evolution of Highly Repetitive DNAs in Sibling Species. *Mol. Biol. Evol.* **2010**, *27*, 1857–1867. [[CrossRef](#)]
66. Mantellatto, A.M.B.; González, S.; Duarte, J.M.B. Molecular Identification of Mazama Species (Cervidae: Artiodactyla) from Natural History Collections. *Genet. Mol. Biol.* **2020**, *43*. [[CrossRef](#)]
67. Escobedo-Morales, L.A.; Mandujano, S.; Eguiarte, L.E.; Rodríguez-Rodríguez, M.A.; Maldonado, J.E. First Phylogenetic Analysis of Mesoamerican Broomtail Deer *Mazama Pandora* and *Mazama Temama* (Cetartiodactyla: Cervidae) Based on Mitochondrial Sequences: Implications for Neotropical Deer Evolution. *Mammal. Biol.* **2016**, *81*, 303–313. [[CrossRef](#)]
68. Heckeberg, N.S. The Systematics of the Cervidae: A Total Evidence Approach. *PeerJ* **2020**, *8*, e8114. [[CrossRef](#)]
69. Carrillo, J.D.; Faurby, S.; Silvestro, D.; Zizka, A.; Jaramillo, C.; Bacon, C.D.; Antonelli, A. Disproportionate Extinction of South American Mammals Drove the Asymmetry of the Great American Biotic Interchange. *Proc. Natl. Acad. Sci. USA* **2020**, *117*, 26281–26287. [[CrossRef](#)]
70. Carrizo, L.V.; Tulli, M.J.; Santos, D.A.D.; Abdala, V. Interplay between Postcranial Morphology and Locomotor Types in Neotropical Sigmodontine Rodents. *J. Anat.* **2014**, *224*, 469–481. [[CrossRef](#)]
71. Pečnerová, P.; Moravec, J.C.; Martínková, N. A Skull Might Lie: Modeling Ancestral Ranges and Diet from Genes and Shape of Tree Squirrels. *Syst. Biol.* **2015**, *64*, 1074–1088. [[CrossRef](#)]
72. Barra, V.; Fachinetti, D. The Dark Side of Centromeres: Types, Causes and Consequences of Structural Abnormalities Implicating Centromeric DNA. *Nat. Commun.* **2018**, *9*, 4340. [[CrossRef](#)]
73. Puppo, I.L.; Saifitdinova, A.F.; Tonyan, Z.N. The Role of Satellite DNA in Causing Structural Rearrangements in Human Karyotype. *Russ. J. Genet.* **2020**, *56*, 41–47. [[CrossRef](#)]
74. Aquino, C.I.; Abril, V.V.; Duarte, J.M.B. Meiotic Pairing of B Chromosomes, Multiple Sexual System, and Robertsonian Fusion in the Red Broomtail Deer *Mazama Americana* (Mammalia, Cervidae). *Genet. Mol. Res. GMR* **2013**, *12*, 3566–3574. [[CrossRef](#)]
75. Abril, V.V.; Duarte, J.M.B. Chromosome Polymorphism in the Brazilian Dwarf Broomtail Deer, *Mazama Nana* (Mammalia, Cervidae). *Genet. Mol. Biol.* **2008**, *31*, 53–57. [[CrossRef](#)]
76. Valeri, P.M.; Tomazella, I.M.; Duarte, J.M.B. Intrapopulation Chromosomal Polymorphism in *Mazama gouazoubira* (Cetartiodactyla; Cervidae): The Emergence of a New Species? *Cytogenet. Genome Res.* **2018**, *154*, 147–152. [[CrossRef](#)]
77. Li, Y.C.; Lee, C.; Sanoudou, D.; Hseu, T.H.; Li, S.Y.; Lin, C.C.; Hsu, T.H. Interstitial Colocalization of Two Cervid Satellite DNAs Involved in the Genesis of the Indian Muntjac Karyotype. *Chrom. Res.* **2000**, *8*, 363–373. [[CrossRef](#)]
78. Yang, F.; O’Brien, P.C.; Wienberg, J.; Neitzel, H.; Lin, C.C.; Ferguson-Smith, M.A. Chromosomal Evolution of the Chinese Muntjac (*Muntiacus reevesi*). *Chromosoma* **1997**, *106*, 37–43. [[CrossRef](#)]
79. Hartmann, N.; Scherthan, H. Characterization of Ancestral Chromosome Fusion Points in the Indian Muntjac Deer. *Chromosoma* **2004**, *112*, 213–220. [[CrossRef](#)]

80. Fiorillo, B.F.; Sarria-Perea, J.A.; Abril, V.V.; Duarte, J.M.B. Cytogenetic Description of the Amazonian Brown Brocket Mazama *Nemorivaga* (Artiodactyla, Cervidae). *Comp. cytogenet.* **2013**, *7*, 25–31. [[CrossRef](#)]
81. Yang, F.; Carter, N.P.; Shi, L.; Ferguson-Smith, M.A. A Comparative Study of Karyotypes of Muntjacs by Chromosome Painting. *Chromosoma* **1995**, *103*, 642–652. [[CrossRef](#)]
82. Yang, F.; O'Brien, P.C.; Wienberg, J.; Ferguson-Smith, M.A. A Reappraisal of the Tandem Fusion Theory of Karyotype Evolution in Indian Muntjac Using Chromosome Painting. *Chrom. Res.* **1997**, *5*, 109–117. [[CrossRef](#)]
83. Ashley, T. X-Autosome Translocations, Meiotic Synapsis, Chromosome Evolution and Speciation. *Cytogenet. Genome Res.* **2002**, *96*, 33–39. [[CrossRef](#)]
84. Cotton, A.M.; Chen, C.-Y.; Lam, L.L.; Wasserman, W.W.; Kobor, M.S.; Brown, C.J. Spread of X-Chromosome Inactivation into Autosomal Sequences: Role for DNA Elements, Chromatin Features and Chromosomal Domains. *Hum. Mol. Genet.* **2014**, *23*, 1211–1223. [[CrossRef](#)]
85. Kalz-Füller, B.; Slegers, E.; Schwanitz, G.; Schubert, R. Characterisation, Phenotypic Manifestations and X-Inactivation Pattern in 14 Patients with X-Autosome Translocations. *Clin. Genet.* **1999**, *55*, 362–366. [[CrossRef](#)]
86. Dobigny, G.; Ozouf-Costaz, C.; Bonillo, C.; Volobouev, V. Viability of X-Autosome Translocations in Mammals: An Epigenomic Hypothesis from a Rodent Case-Study. *Chromosoma* **2004**, *113*, 34–41. [[CrossRef](#)]
87. Ratomponirina, C.; Viegas-Péquignot, E.; Dutrillaux, B.; Petter, F.; Rumpler, Y. Synaptonemal Complexes in Gerbillidae: Probable Role of Intercalated Heterochromatin in Gonosome-Autosome Translocations. *Cytogenet. Cell Genet.* **1986**, *43*, 161–167. [[CrossRef](#)] [[PubMed](#)]
88. Vozdova, M.; Ruiz-Herrera, A.; Fernandez, J.; Cernohorska, H.; Frohlich, J.; Sebestova, H.; Kubickova, S.; Rubes, J. Meiotic Behaviour of Evolutionary Sex-Autosome Translocations in Bovidae. *Chrom. Res.* **2016**, *24*, 325–338. [[CrossRef](#)] [[PubMed](#)]
89. Camacho, J.P.; Sharbel, T.F.; Beukeboom, L.W. B-Chromosome Evolution. *Philos. Trans. R. Soc. Lond. B Biol. Sci.* **2000**, *355*, 163–178. [[CrossRef](#)] [[PubMed](#)]
90. Trifonov, V.A.; Dementyeva, P.V.; Larkin, D.M.; O'Brien, P.C.M.; Perelman, P.L.; Yang, F.; Ferguson-Smith, M.A.; Graphodatsky, A.S. Transcription of a Protein-Coding Gene on B Chromosomes of the Siberian Roe Deer (*Capreolus pygargus*). *BMC Biol.* **2013**, *11*, 90. [[CrossRef](#)] [[PubMed](#)]
91. Duke Becker, S.E.; Thomas, R.; Trifonov, V.A.; Wayne, R.K.; Graphodatsky, A.S.; Breen, M. Anchoring the Dog to Its Relatives Reveals New Evolutionary Breakpoints across 11 Species of the Canidae and Provides New Clues for the Role of B Chromosomes. *Chrom. Res.* **2011**, *19*, 685–708. [[CrossRef](#)]
92. Makunin, A.I.; Kichigin, I.G.; Larkin, D.M.; O'Brien, P.C.M.; Ferguson-Smith, M.A.; Yang, F.; Proskuryakova, A.A.; Vorobieva, N.V.; Chernyaeva, E.N.; O'Brien, S.J.; et al. Contrasting Origin of B Chromosomes in Two Cervids (Siberian Roe Deer and Grey Brocket Deer) Unravalled by Chromosome-Specific DNA Sequencing. *BMC Genom.* **2016**, *17*, 618. [[CrossRef](#)]